This paper has proposed a program analysis method over the current state of the workspace of an anthropomorphic manipulator using the Mathcad software application package (USA). The analysis of the manipulator workspace helped solve the following sub-tasks: to calculate the limits of the grip reach, to determine the presence of "dead zones" within the manipulator workspace, to build the boundaries of the manipulator workspace. A kinematic scheme of the manipulator typically provides for at least five degrees of mobility, which is why in the three-dimensional Cartesian coordinate system the work zone boundaries represent the surfaces of a complex geometric shape. The author-devised method makes it possible to construct the projections of the boundaries of the manipulator's work zone onto the coordinate planes in the frame of reference associated with the base of the robot.

Using Mathcad's built-in features makes it possible to effectively solve the above sub-tasks without wasting time developing specialized software. The Mathcad software application package provides for the possibility of a symbolic solution to the first problem of the kinematics of an industrial robot, that is, the program generates analytical dependences of the coordinates for special point P (pole) of the grip on the trigonometrical functions of the generalized coordinates. The resulting analytical dependences are used for kinematic and dynamic analysis of the manipulator.

Special features in constructing mathematical models when using the Mathcad software application package have been revealed. Simulating the manipulator movement taking into consideration constraints for kinematic pairs, the drives' power, as well as friction factors, makes it possible to optimize the parameters of the manipulator kinematic scheme.

An example of the analysis of the working space of an anthropomorphic manipulator with five degrees of mobility has been considered.

The reported results could be used during the design, implementation, modernization, and operation of manipulators

Keywords: kinematic scheme, grab pole, coordinate conversion, workspace, reach limits

DEVISING A METHOD TO ANALYZE THE CURRENT STATE OF THE MANIPULATOR WORKSPACE

N. Ashhepkova
PhD,
Associate Professor
Department of Mechanotronics
Oles Honchar Dnipro
National University
Gagarina ave., 72, Dnipro,
Ukraine, 49010
E-mail: ashchepkovanatalya@gmail.com

1. Introduction

The development of engineering and information technologies leads to the use of robots not only in the industry but also for military purposes, medicine, agriculture, to eliminate the consequences of anthropogenic and natural disasters, etc. The structure of a robot is often based on the assembly-modular principle and consists of a self-propelled platform and attached equipment (manipulator, probe, drill, etc.). A wide range of structural elements and sensors makes it possible to construct models with different types of chassis, manipulators, and grippers; as well as to implement different control algorithms and movement laws.

The proliferation of collaborative robotics implies the presence of a human within the workspace of the manipulator, as well as their dynamic interaction. To ensure full human safety, the robot's control system must analyze the current state of its workspace, namely:

– to timely recognize and identify a person as a moving obstacle within the manipulator workspace;

– to analyze the possibility of the manipulator continuing to perform programmed movements and technological operations;

– to calculate the coordinates of those points within the workspace at which the person is, which are not allowed for the manipulator;

– to calculate changes in the region of allowable values of the manipulator's generalized coordinates (kinematic pairs);

– to define the valid configurations of the manipulator to successfully complete technological operations under the identified limitations;

– to synthesize the law of change in the generalized coordinates for the successful completion of technological operations with acceptable values of the kinematic and dynamic parameters.

The safety requirements for systems involving a collaborating robot in accordance with ISO 10218 should be revised by May 2021.

For the effective interaction between a group of robots and technological equipment, or a person, or the environment, or each other, it is also necessary to analyze the current state of the manipulators' working space according to some software algorithm.

When using manipulative mobile robots (MR) in a previously unknown environment, timely detection of obstacles and appropriate correction of the manipulator's programmed movements improves the survivability of the structure and ensures the success of the mission. Indeed, in eliminating the consequences of anthropogenic and natural disasters, at reconnaissance and demining, the working space of the MR manipulator may be limited (for example, the width of the opening). This predetermines a change in the set of val-

ues of the generalized coordinates and limits of grip reach, narrowing the size of the workspace, reducing the number of acceptable configurations of the manipulator, decreasing the accuracy of positioning. Neglecting the above limitations under conditions of autonomous operation and remote control could lead to a loss of MR functionality.

The relevance of the current work is related to the need to devise a method for program analysis of the current state of manipulators' workspaces in the presence of constraints. The analysis of the current state of the manipulator's workspace implies calculating the limits of the grip reach, determining the presence of "dead zones" within the workspace of the manipulator, building the boundaries of the manipulator's workspace. Based on the data obtained, the movement of the manipulator is simulated taking into consideration constraints in the kinematic pairs, drives' power, as well as friction factors. This would make it possible to determine the acceptable configurations of the manipulator, synthesize the optimal trajectory, successfully complete technological operations, and preserve the functionality of the robot despite the existence of restrictions and obstacles within its workspace.

2. Literature review and problem statement

The instability of the economy forces entrepreneurs to modernize production by expanding the range of manufactured goods, by applying new materials and technologies. At the same time, robots provide for the high performance, the accuracy of repetitive operations, the low percentage of defects, minimum time to reconfigure the production for a new product [1].

The complexity of technological operations, work within a limited space, the dynamic interaction of several manipulators lead to the need to analyze the workspace of industrial robots (IR) not only when they are introduced into production but also during operation. The authors of [1], for example, studied the rigidity characteristics of the robot Kuka KR 500 and identified those areas within the workspace where the least load is applied to the manipulator's gripper drives, thereby meeting the stricter requirements for the accuracy of milling. The task of finding a safe working space (SWS) for a robot involved in the maintenance and monitoring of electrical substations was considered in [3]. Being the basic material for robots, metal significantly changes the intensity and distribution of an electric field at positioning to a working configuration and during operation. The authors gave a method of calculating the safe working space of the manipulator in a heterogeneous electric field, thereby preventing an interphase breakdown or breakdown between the phase and the ground. That ensures the safety of the human operator, the reliability and economic efficiency of the substation. The authors of [4] analyzed the limits of reach by the robot involved in cotton palette stacking. They applied a graph-analytical method to derive a curvilinear motion equation in the *XOY* plane, calculated the limits of the robot's wrist reach, and determined the finish area within the robot's workspace. That improves the accuracy of positioning accuracy, as well as loading operation performance. Therefore, analyzing a workspace during IR operation could reveal reserves to improve the productivity and quality of the technological process.

Typically, the occurrence of an obstacle inside the fenced workspace when moving the IR manipulator blocks the execution of programmed movements. After removing obstacles and interference, the operator restarts the process cycle. However, modern adaptive robots can identify obstacles within their workspace based on the information from video cameras, beacons [6], etc. The synthesis of the trajectory that bypasses obstacles is conducted by the robot control system based on the analysis of a digital model of the current state of the workspace.

Paper [5] states that increasing the speed at which objects move within the IR workspace leads to that the time required to build a workspace model is often commensurate, and sometimes longer, than the time it takes to perform a process operation. The cited paper proposes a method of forming a three-dimensional model of the current state of an IR workspace based on information acquired from a stereoscopic system. However, the technical limitations of video cameras and the lack of light over the workspace lead to the appearance of halos, shadows, highlights, etc. on the image.

Article [6] examines the algorithm of targeting the led MR in an unknown environment by the acoustic signal from a stationary beacon or a beacon of the drive vehicle. The features of the bearing and filtering the signal in the presence of noise are analyzed. The authors point out that the identification of the coordinates of the drive robot and the formation of a model of the workspace is possible when at least three beacons interact.

The methods proposed in [5, 6] imply additional costs for processing primary information from sensors, have a significant lag, and could lead to significant errors in determining the actual distances to obstacles. Such methods to build a model of the current state of manipulators' workspace do not warrant the optimal trajectory, the absence of collisions, and maintaining a robot's functionality.

If the robot needs to interact with an object whose position and orientation are set at some space point M, then, when planning the movements, it is necessary to check that the point M is reachable, and that there are alternatives to the acceptable configurations of the manipulator at this point, and that there is a possibility to enable the orientation of the grip to capture and hold the object during programmed movements. Study [7] proposes an algorithm that sets the required orientation of the manipulator grip within the selected space of the Cartesian coordinates. The authors considered 54 orientation-setting techniques based on the 3×3 turn matrix, and six based on Euler's angles. The reported techniques make it easier to pair coordinate systems associated with the subject of manipulation and the working body of the robot's manipulator. However, there remain unresolved issues related to determining which of the considered grip orientation techniques could be enabled by the manipulator's acceptable configurations. In addition, in order to hold an object and alter its orientation at manipulating, it is necessary to determine the acceptable regions of values for the generalized coordinates and the power of the drives.

The trajectory synthesis and the selection of acceptable manipulator configurations are based on a digital model of the current state of the workspace. This leads to the need to find new, more effective methods to build a digital model of the manipulator's workspace. The authors of [8] applied the Monte Carlo method to simulate the workspace of a service

robot manipulator with five degrees of freedom. The efficiency of the workspace model was confirmed by the numerical modeling in MATLAB.

The presence of obstacles within the workspace of a manipulator complicates the task of selecting acceptable configurations and the synthesis of grip trajectories. The authors of [9] consider an algorithm for controlling an *n*-link manipulative robot in an environment with unknown static obstacles. A theorem is proved that claims that by moving on this algorithm within a discrete configuration space the manipulative robot would, over the finite number of steps, either capture the object or give a reasonable answer that the object cannot be captured in any of the configurations. The results of further research were reported in [10]. The advanced algorithm functions in continuous configuration space; the number of obstacles is arbitrary, as well as their shape and location. It is shown that trajectory synthesis is reduced to solving the finite number of road planning tasks in an environment with known prohibited states. A manipulator given in [10] is equipped with a sensor system that could deliver unreliable information about the environment. That leads to the need to verify primary information from sensors, reduces performance, and could lead to collisions.

Paper [11] explores motion planning for robotic manipulators within a single-RRT-based space and a bi-RRT solution tree. The target configuration in the standard bi-RRT is replaced in the new algorithm by a group of acceptable configurations. To determine acceptable and targeted configurations, an algorithm is used to solve the inverse problem of kinematics at the designated points of the workspace. Within a workspace with the predefined obstacles, one of the valid configurations is automatically selected to ensure the optimal grip trajectory. This method requires significant computational costs to determine at each iteration of the target configuration from a set of valid ones.

The authors of [12] propose a technique to set acceptable configurations and synthesize trajectories using a 3D model. The operator sees the movement of the model on a miniature screen of transparent glasses and visually controls the workspace, for timely maneuvering, making it possible to avoid collisions. When programming the movements of the manipulator, the operator uses an eye, intuition, and experience. When interference to the movement of the manipulator emerges, the operator should ensure a quick reaction, the effectiveness of control influences, a minimum probability of collisions, and a high accuracy of analysis of the current state of the workspace in the presence of constraints. In a given case, the optimal trajectory depends on the skill of the operator.

To improve maneuverability and ensure the evasion of the manipulator from moving obstacles in the workspace, it is advisable to use manipulators on a mobile base or manipulative MR. The authors of [13] report the results of simulating the movement of the "Varan" MR manipulator in the implementation of the obstacle detection and collision prevention algorithm. They devised a parametric technique to set a totality of cross-sections that assign the shape and position of the region of permitted configurations at the different locations of forbidden zones. The analytical dependences derived in [14] make it possible to set the region of permitted configurations, which is a knowledge base for the intelligent control over the movement of the arm mechanism within a predefined external environment. The novelty of the research is the use of the region of permitted configu-

rations in the synthesis of trajectory within the space of the generalized coordinates, which makes it possible to correct the movement of the android robot's arm in order to anticipate and eliminate dead-end situations in the synthesis of movements on the velocity vector. The authors of [13, 14] devised a parametric technique to set the region of permitted configurations used for the intelligent motion control of the MR manipulator mechanism within a predefined external environment. However, the issues related to the detection of obstacles and the prevention of collisions in an unknown external environment remained unresolved.

Article [15] solved a direct positional problem to determine the work area and assess the functionality of a manipulative MR. Combining a mobile platform with omni-wheels and the manipulator could significantly expand the service area and improve the functionality of the robot but it reduces the accuracy of grip positioning. In addition, the proposed design of the MR manipulator with three degrees of mobility does not provide for the set of acceptable configurations for each point of the workspace and reduces the service ratio.

The TCMP (Task-constrained motion planning) for the collaborative MR manipulator is explored in [16]. The authors consider the interaction of the robot and human as a movement of the manipulator within the workspace with moving obstacles. To synthesize the law of control, a model is proposed to maximize the minimum distance between the obstacles and MR and, at the same time, to minimize the speed at the points of touch. Using sensor information and speed-adjusted control, MR could move away from approaching people, with a wrist fixed to complete a technological operation (tool manipulation).

The presence of a mobile base improves the maneuverability of manipulative MR, expands the working space, and increases the number of acceptable configurations of the manipulator, but reduces the accuracy of (tool) grip positioning.

The problem of synthesis of trajectory control over the movement of MR in the presence of external moving objects within the working space was investigated in [17]. To solve the problem of the relative dynamics of the MR and an external mobile object, the authors built proportional-differential control algorithms with direct compensation of non-linearities. The trajectory synthesis is based on a digital model of the current state of the workspace. The example implies bypassing the external moving object on a circular trajectory and returning to the original desired straight trajectory. However, the authors of [17] do not give an estimate of the optimality of the circular trajectory of the bypass maneuver.

Contact operations are considered in [18], where the robot's gripping device is in direct contact with objects in the external environment. The authors solve the problem of minimizing the risk of damage to the technological tool and violation of the processing regime. This could be achieved by having data on the position of the object in space relative to the end link (grip) of the manipulator and the geometric parameters of the object. The cited article examines approaches to the reconstruction of the surface of an object located in the manipulator's work area, on the basis of a cloud of points; the authors also proposed a method to describe the object with rotation surfaces based on a noisy and incomplete cloud of points, acquired from a stereoscopic system installed on the manipulator's end link. However, the authors do not assess the conformity of the shape and size of actual obstacles

and the reconstruction of the surface of the object located within the working area of the manipulator.

The development of a programming method to analyze the current state of the manipulator's workspace in the presence of obstacles or constraints in the kinematic pairs and drives could make it possible:

– to build a digital model of the workspace;

– to assess the limits of the manipulator's reach if there are constraints in the kinematic pairs and drives;

– to synthesize an optimal trajectory with acceptable manipulator configurations;

– to avoid colliding with a person or an obstacle.

The above analysis of the scientific literature suggests that devising a programming method to analyze the current state of the manipulator's workspace in the presence of obstacles or constraints in the kinematic pairs and drives could resolve an issue related to maintaining the functionality of the manipulator and preventing collisions.

3. The aim and objectives of the study

The aim of this study is to develop a programming method to analyze the current state of the manipulator's workspace in the presence of obstacles or constraints in the kinematic pairs and drives.

That would make it possible to identify reserves for improving the productivity and quality of the technological process for IR manipulators, ensuring the safe interaction of humans with the manipulator of collaborative robots, and improving the efficiency and survivability of manipulative MR in eliminating the consequences of anthropogenic and natural disasters.

To accomplish the aim, the following tasks have been set:

– to define the laws of change in the generalized coordinates $q_i(t)$ taking into consideration constraints in the kinematic pairs, the power of drives, and friction factors;

– to calculate the limits of grip reach, that is, to compute the minimum and maximum distance for special point P in the frame of reference associated with the base of the robot;

– to build the boundaries of the manipulator's workspace and identify the presence of "dead zones" within it.

4. Materials and methods to solve the sub-tasks in analyzing the workspace of a manipulator

4. 1. Manipulator design and initial conditions

A universal anthropomorphic robotic manipulator is a simplified kinematic prototype of a human arm. The structure of the universal manipulator has at least 4 controlled degrees of mobility and ends with a flank to attach a manufacturing tool [1]. The initial data for the design of the manipulator are [19, 20]:

– the kinematic manipulator scheme;

– the geometric dimensions of the manipulator links;

– the permissible laws of change in the generalized coordinates of the manipulator;

– the initial position of the links;

– the structural constraints in the kinematic pairs of the manipulator;

– load information.

An example chosen here is the structure of a manipulator with five rotary kinematic pairs of class 5. It was assumed that the mass of the kinematic pairs could be disregarded while the links of the manipulator were absolutely rigid hard rods with an even distribution of mass. The kinematic scheme of the manipulator is shown in Fig. 1.
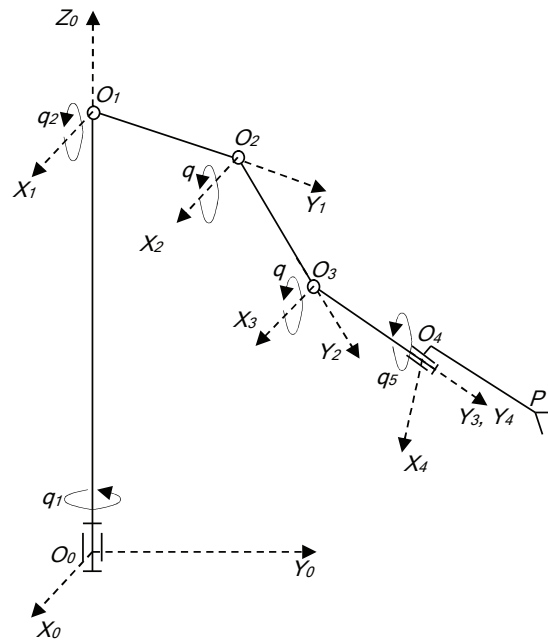
Fig. 1. Kinematic scheme of the manipulator

The following is adopted for calculation:

– the laws of change in generalized coordinates

$$q_1(t) = 0.5\frac{t^2}{2} - 0.03t + \frac{\pi}{4},$$

$$q_2(t) = q_3(t) = q_4(t) = 0.3\frac{t^2}{2} - 0.03t + \frac{\pi}{6},$$

$$q_5(t) = 0.3\frac{t^2}{2} - 0.05t + \frac{\pi}{6};$$

– the initial values of generalized coordinates

$$q_{10} = q_1(0) = \frac{\pi}{4},$$

$$q_{20} = q_2(0) = \frac{\pi}{6},$$

$$q_{30} = q_3(0) = \frac{\pi}{6},$$

$$q_{40} = q_4(0) = \frac{\pi}{6},$$

$$q_{50} = q_5(0) = \frac{\pi}{6};$$

– the regions to determine the generalized coordinates

$$q_1(t) \in \left[\frac{\pi}{180}; \frac{15\pi}{8}\right],$$

$$q_2(t) \in \left[\frac{\pi}{180}; \frac{2\pi}{3}\right],$$

$$q_3(t) \in \left[\frac{\pi}{180}; \frac{2\pi}{3}\right],$$

$$q_4(t) \in \left[\frac{\pi}{180}; \frac{2\pi}{3}\right],$$

$$q_5(t) \in \left[\frac{\pi}{180}; \frac{15\pi}{8}\right];$$

– the P coordinates (0.05; 0.3; 0) of the gripping capacity pole at the initial point in time in the $X_4 Y_4 Z_4$ system.

4. 2. Software

To solve problems related to the current analysis of the manipulator's workspace, the Mathcad software application package was employed. The effectiveness of Mathcad application when solving the problems of kinematic and dynamic analysis, the simulation of the manipulator's movement, the synthesis and analysis of the trajectories of IR grip was proven in [19].

The Mathcad software application package provides for the possibility of a symbolic solution to the first problem of the kinematics of an industrial robot, that is, the software generates the analytical dependences of the coordinates for special point P (the pole) of the grip on the trigonometrical functions of the generalized coordinates. The resulting analytical dependences were used for the kinematic analysis of the manipulator [19].

4. 3. Theoretical methods

To solve the problem on the position of a special point P (the pole) of the grip, the conversion of coordinates by the Denavit-Hartenberg method [19, 20] was applied.

To determine the permissible laws of change in generalized coordinates, I have developed a software module in the Mathcad environment and used the graph-analytic method [21].

To reduce the error and eliminate the subjectivity of the assessment, the limits of the grip reach (the limits of distance for special point P) were calculated in several ways to verify the results: by using methods to find an extremum of the unimodal functions (a dichotomy method, a method of the golden section), and by applying the tracing for graphs $x_p^0(t)$, $y_p^0(t)$, $z_p^0(t)$ [21].

The presence of "dead zones" was determined by using differential calculus methods [22].

To build the boundary of the manipulator's workspace, I have developed a software module in the Mathcad environment and used the orthogonal design method [21, 22].

5. Results of studying the manipulator's workspace using Mathcad

5. 1. Determining the laws of change in the generalized coordinates $q_i(t)$ considering the constraints

The kinematic scheme of the manipulator is shown in Fig. 1:

1) Each link of the manipulator is associated with the right-hand Cartesian coordinate system $O_i X_i Y_i Z_i$. The origin of the countdown O_i is located in the center of the kinematic pair; one coordinate axis runs along the axis of the hinge rotation; the second coordinate axis runs along the axis of the link symmetry; the third coordinate axis complemented the system to the right-hand one [19, 20, 22].

2) The Denavit-Hartenberg coordinate conversion matrices were built [19, 20, 22] for the example under consideration:

$$A_4^5 = \begin{bmatrix} \cos q_5(t) & 0 & \sin q_5(t) & 0 \\ 0 & 1 & 0 & 0 \\ -\sin q_5(t) & 0 & \cos q_5(t) & 0 \\ 0 & 0 & 0 & 1 \end{bmatrix},$$

$$A_3^4 = \begin{bmatrix} 1 & 0 & 0 & 0 \\ 0 & \cos q_4(t) & \sin q_4(t) & 34 \\ 0 & -\sin q_4(t) & \cos q_4(t) & 0 \\ 0 & 0 & 0 & 1 \end{bmatrix},$$

$$A_2^3 = \begin{bmatrix} 1 & 0 & 0 & 0 \\ 0 & \cos q_2(t) & \sin q_2(t) & 23 \\ 0 & -\sin q_2(t) & \cos q_2(t) & 0 \\ 0 & 0 & 0 & 1 \end{bmatrix},$$

$$A_1^2 = \begin{bmatrix} 1 & 0 & 0 & 0 \\ 0 & \cos q_2(t) & \sin q_2(t) & 12 \\ 0 & -\sin q_2(t) & \cos q_2(t) & 0 \\ 0 & 0 & 0 & 1 \end{bmatrix},$$

$$A_0^1 = \begin{bmatrix} \cos q_1(t) & \sin q_1(t) & 0 & 0 \\ -\sin q_1(t) & \cos q_1(t) & 0 & 0 \\ 0 & 0 & 1 & c_{01} \\ 0 & 0 & 0 & 1 \end{bmatrix}.$$

3) Based on the kinematic diagram of the manipulator, the movement of special point P was represented as a sequence of movements along each generalized coordinate. A chain of movements was compiled, from link 0 (the base of the manipulator) to link 5, relative to which special point P is stationary.

$$0 \xrightarrow{A_w(\vec{k}, q_1)} 1 \xrightarrow{A_w(\vec{i}, q_2)} 2 \xrightarrow{A_w(\vec{i}, q_3)} 3 \xrightarrow{A_w(\vec{i}, q_4)} 4 \xrightarrow{A_w(\vec{j}, q_5)} 5,$$

in this case,

$$A_0^1 = A_w\left(\vec{k}, q_1\right),\ A_1^2 = A_w\left(\vec{i}, q_2\right),\ A_2^3 = A_w\left(\vec{i}, q_3\right),$$

$$A_3^4 = A_w\left(\vec{i}, q_4\right),\ A_4^5 = A_w\left(\vec{j}, q_5\right).$$

4) A matrix equation was constructed to calculate the coordinates for point P of the manipulator in the base-related reference system:

$$\vec{r}_P^0 = A_0^1 \cdot A_1^2 \cdot A_2^3 \cdot A_3^4 \cdot A_4^5 \cdot \vec{r}_P^5 = T_5 \cdot \vec{r}_P^5,$$

where $\vec{r}_P^0 = \left(x_p^0 \quad y_p^0 \quad z_p^0 \quad 1\right)^T$ are the coordinates of point P in the manipulator base-related reference system; $T_5 = A_0^1 \cdot A_1^2 \cdot A_2^3 \dots A_{n-1}^n$ is the general matrix that converts coordinates from the n-th link to link 0 (in the manipulator base); $\vec{r}_P^5 = \left(x_p^5 \quad y_p^5 \quad z_p^5 \quad 1\right)^T$ are the coordinates of point P in the frame of reference associated with the fifth link of the IR manipulator.

5) The matrices were treated as follows:

$$
\vec{r}_P^0 =
\begin{bmatrix}
\cos q_1(t) & \sin q_1(t) & 0 & 0 \\
-\sin q_1(t) & \cos q_1(t) & 0 & 0 \\
0 & 0 & 1 & c_{01} \\
0 & 0 & 0 & 1
\end{bmatrix}
\cdot
\begin{bmatrix}
1 & 0 & 0 & 0 \\
0 & \cos q_2(t) & \sin q_2(t) & c_{12} \\
0 & -\sin q_2(t) & \cos q_2(t) & 0 \\
0 & 0 & 0 & 1
\end{bmatrix}
\times
$$

$$
\times
\begin{bmatrix}
1 & 0 & 0 & 0 \\
0 & \cos q_2(t) & \sin q_2(t) & c_{23} \\
0 & -\sin q_2(t) & \cos q_2(t) & 0 \\
0 & 0 & 0 & 1
\end{bmatrix}
\cdot
\begin{bmatrix}
1 & 0 & 0 & 0 \\
0 & \cos q_4(t) & \sin q_4(t) & c_{34} \\
0 & -\sin q_4(t) & \cos q_4(t) & 0 \\
0 & 0 & 0 & 1
\end{bmatrix}
\cdot
$$

$$
\cdot
\begin{bmatrix}
\cos q_5(t) & 0 & \sin q_5(t) & 0 \\
0 & 1 & 0 & 0 \\
-\sin q_5(t) & 0 & \cos q_5(t) & 0 \\
0 & 0 & 0 & 1
\end{bmatrix}
\cdot
\begin{bmatrix}
x_P^5 \\
y_P^5 \\
0 \\
1
\end{bmatrix}.
$$

6) I have compiled a program to model the laws of change in generalized coordinates. Features of the kinematic pair's design impose restrictions on the region of values corresponding to the generalized coordinate $q_i(t) \in [q_{i\,min}; q_{i\,max}]$. Fig. 2, a shows a fragment of the program that models the law of change in the generalized coordinate $q_3(t)$ taking the constraints into consideration. The drive of the highlighted degree of mobility generates an increase in the generalized coordinate according to the following law

$$
Q_3(t) = \frac{0.3 \cdot t^2}{2} - 0.03t + \frac{\pi}{6}.
$$

The actual implementation of $q_3(t)$ takes into consideration features in the design of the kinematic pair and the $q_3(t) \in \left[\dfrac{\pi}{180}; \dfrac{2\pi}{3}\right]$. constraints. The diagrams of change in the estimated $Q_3(t)$ and actual $q_3(t)$ values of the generalized coordinate are shown in Fig. 2, b.

Fig. 3 shows a fragment of the program to model the laws of change in the manipulator's generalized coordinates taking into consideration the predefined constraints in the kinematic pairs, the power of drives, and friction factors. The modeling was performed under the following initial conditions: the laws of change in the generalized coordinates

$$
q_1(t) = 0.5\frac{t^2}{2} - 0.03t + \frac{\pi}{4},
$$

$$
q_2(t) = q_3(t) = q_4(t) = 0.3\frac{t^2}{2} - 0.03t + \frac{\pi}{6},
$$

$$
q_5(t) = 0.3\frac{t^2}{2} - 0.05t + \frac{\pi}{6};
$$

the initial values of the generalized coordinates

$$
q_{10} = q_1(0) = \frac{\pi}{4}, \quad q_{20} = q_2(0) = \frac{\pi}{6}, \quad q_{30} = q_3(0) = \frac{\pi}{6},
$$

$$
q_{40} = q_4(0) = \frac{\pi}{6}, \quad q_{50} = q_5(0) = \frac{\pi}{6}
$$

and limiting the values of the generalized coordinates

$$
q_1(t) \in \left[\frac{\pi}{180}; \frac{15\pi}{8}\right], \quad q_2(t) \in \left[\frac{\pi}{180}; \frac{2\pi}{3}\right], \quad q_3(t) \in \left[\frac{\pi}{180}; \frac{2\pi}{3}\right],
$$

$$
q_4(t) \in \left[\frac{\pi}{180}; \frac{2\pi}{3}\right], \quad q_5(t) \in \left[\frac{\pi}{180}; \frac{15\pi}{8}\right].
$$

$$
\text{Q3\_0} := \frac{\pi}{6}
$$

$$
\text{Q3\_min} := \frac{\pi}{180} \quad \text{Q3\_max} := 2 \cdot \frac{\pi}{3}
$$

$$
\text{Q3(t)} := \frac{a3 \cdot t^2}{2} + b3 \cdot t + \text{Q3\_0}
$$

$$
\text{q3(t)} := \begin{cases} \text{Q3\_max} & \text{if } \text{Q3(t)} \geq \text{Q3\_max} \\ \text{Q3\_min} & \text{if } \text{Q3(t)} \leq \text{Q3\_min} \\ \text{Q3(t)} & \text{otherwise} \end{cases}
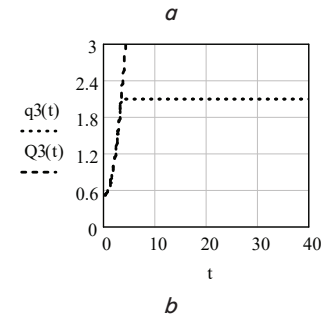$$

a

b

Fig. 2. Modeling the law of change in the generalized coordinate $q_3(t)$ taking the constraints into consideration: a – fragment of the program modeling the law of change in the generalized coordinate $q_3(t)$ taking the constraints into consideration; b – charts of change in the estimated $Q_3(t)$ and actual $q_3(t)$ values of the generalized coordinate

```
origin := 1  t0 := 0  tk := 40  dt := 0.1  t := 0, 0.1 .. tk
.dovgina_lank  x5 := 0.05  y5 := 0.3  z5 := 0
c01 := 0.05  c12 := 0.8  c23 := 0.7  c34 := 0.6
.parametru_privodiv
a1 := 0.5  a2 := 0.3  a3 := 0.3  a4 := 0.3  a5 := 0.3
b1 := −0.03  b2 := −0.03  b3 := −0.03  b4 := −0.03  b5 := −0.05
.oblast_vuznachennya
```

$$
\text{Q1\_min} := \frac{\pi}{180} \quad \text{Q2\_min} := \frac{\pi}{180} \quad \text{Q3\_min} := \frac{\pi}{180} \quad \text{Q4\_min} := \frac{\pi}{180} \quad \text{Q5\_min} := \frac{\pi}{180}
$$

$$
\text{Q1\_max} := 15 \cdot \frac{\pi}{8} \quad \text{Q2\_max} := 2 \cdot \frac{\pi}{3} \quad \text{Q3\_max} := 2 \cdot \frac{\pi}{3} \quad \text{Q4\_max} := 2 \cdot \frac{\pi}{3} \quad \text{Q5\_max} := 15 \cdot \frac{\pi}{8}
$$

.zakon_ruhu

$$
\text{Q1\_0} := \frac{\pi}{4} \quad \text{Q2\_0} := \frac{\pi}{6} \quad \text{Q3\_0} := \frac{\pi}{6} \quad \text{Q4\_0} := \frac{\pi}{6} \quad \text{Q5\_0} := \frac{\pi}{6}
$$

$$
\text{Q1(t)} := \frac{a1 \cdot t^2}{2} + b1 \cdot t + \text{Q1\_0} \quad \text{Q2(t)} := \frac{a2 \cdot t^2}{2} + b2 \cdot t + \text{Q2\_0}
$$

$$
\text{Q3(t)} := \frac{a3 \cdot t^2}{2} + b3 \cdot t + \text{Q3\_0} \quad \text{Q4(t)} := \frac{a4 \cdot t^2}{2} + b4 \cdot t + \text{Q4\_0}
$$

$$
\text{Q5(t)} := \frac{a5 \cdot t^2}{2} + b5 \cdot t + \text{Q5\_0}
$$

$$
\text{q1(t)} := \begin{cases} \text{Q1\_max} & \text{if } \text{Q1(t)} \geq \text{Q1\_max} \\ \text{Q1\_min} & \text{if } \text{Q1(t)} \leq \text{Q1\_min} \\ \text{Q1(t)} & \text{otherwise} \end{cases} \quad \text{q2(t)} := \begin{cases} \text{Q2\_max} & \text{if } \text{Q2(t)} \geq \text{Q2\_max} \\ \text{Q2\_min} & \text{if } \text{Q2(t)} \leq \text{Q2\_min} \\ \text{Q2(t)} & \text{otherwise} \end{cases}
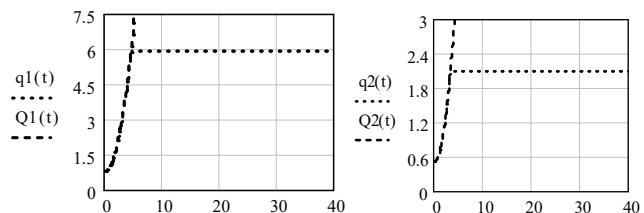$$

Fig. 3. Modeling the laws of change in the manipulator's generalized coordinates under the predefined initial conditions

5. 2. Calculating the limits of the grip reach in the frame of reference associated with the robot's base

1) The software was developed that makes it possible to simulate the movements of the manipulator for different laws

of change in generalized coordinates taking into consideration the power of the drive, friction factors, design features, and the characteristics of kinematic pairs.

Fig. 4 shows the results of simulating the movement of the pole of the manipulator's grip under the predefined constraints in the generalized coordinates $q_i(t) \in [q_{i\,min};\ q_{i\,max}]$, $i=1,...,5$ using the Mathcad software application package.

.matricu_peretvorennya

$$A10(t) := \begin{pmatrix} \cos(q1(t)) & \sin(q1(t)) & 0 & 0 \\ -\sin(q1(t)) & \cos(q1(t)) & 0 & 0 \\ 0 & 0 & 1 & c01 \\ 0 & 0 & 0 & 1 \end{pmatrix} \quad A21(t) := \begin{pmatrix} 1 & 0 & 0 & 0 \\ 0 & \cos(q2(t)) & \sin(q2(t)) & c12 \\ 0 & -\sin(q2(t)) & \cos(q2(t)) & 0 \\ 0 & 0 & 0 & 1 \end{pmatrix}$$

$$A32(t) := \begin{pmatrix} 1 & 0 & 0 & 0 \\ 0 & \cos(q3(t)) & \sin(q3(t)) & c23 \\ 0 & -\sin(q3(t)) & \cos(q3(t)) & 0 \\ 0 & 0 & 0 & 1 \end{pmatrix} \quad A43(t) := \begin{pmatrix} 1 & 0 & 0 & 0 \\ 0 & \cos(q4(t)) & \sin(q4(t)) & c34 \\ 0 & -\sin(q4(t)) & \cos(q4(t)) & 0 \\ 0 & 0 & 0 & 1 \end{pmatrix}$$

$$A54(t) := \begin{pmatrix} \cos(q5(t)) & 0 & \sin(q5(t)) & 0 \\ 0 & 1 & 0 & 0 \\ -\sin(q5(t)) & 0 & \cos(q5(t)) & 0 \\ 0 & 0 & 0 & 1 \end{pmatrix}$$

.koordunatu_polyusu $\quad R\_P(t) := A10(t) \cdot A21(t) \cdot A32(t) \cdot A43(t) \cdot A54(t) \cdot PP$

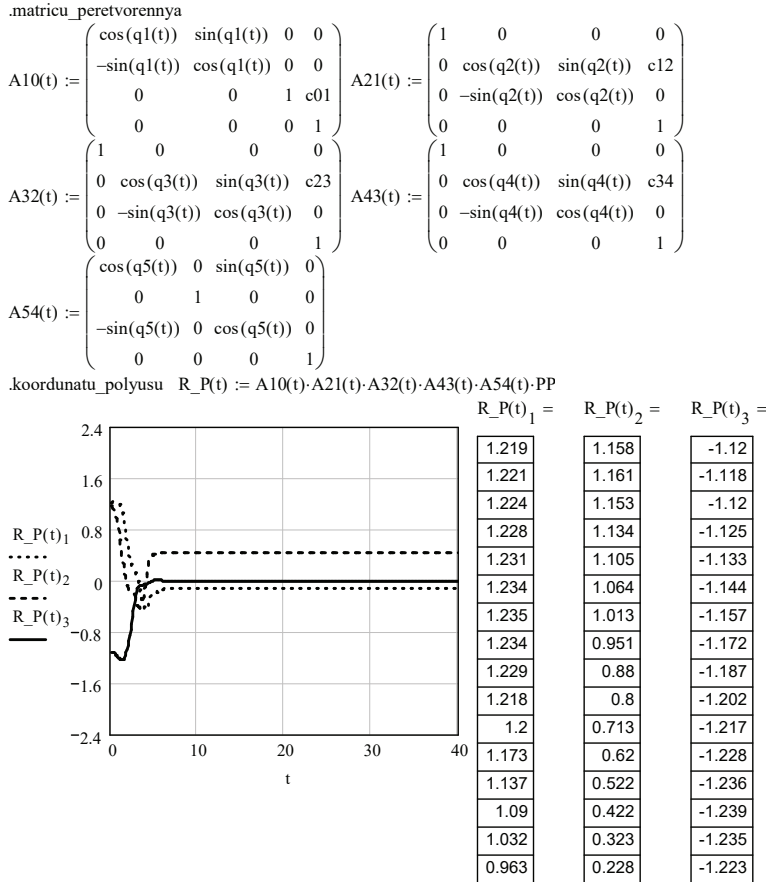| $R\_P(t)_1 =$	$R\_P(t)_2 =$	$R\_P(t)_3 =$
1.219	1.158	-1.12
1.221	1.161	-1.118
1.224	1.153	-1.12
1.228	1.134	-1.125
1.231	1.105	-1.133
1.234	1.064	-1.144
1.235	1.013	-1.157
1.234	0.951	-1.172
1.229	0.88	-1.187
1.218	0.8	-1.202
1.2	0.713	-1.217
1.173	0.62	-1.228
1.137	0.522	-1.236
1.09	0.422	-1.239
1.032	0.323	-1.235
0.963	0.228	-1.223

Fig. 4. Modeling the movement of the pole of the manipulator's grip under the predefined constraints in the generalized coordinates $q_i(t) \in [q_{i\,min};\ q_{i\,max}]$, $i=1,...,5$ using the Mathcad software application package

3) To find the highest and smallest values for the coordinates of special point P, subprograms have been developed to compute an extremum of the functions f_x, f_y, f_z by a dichotomy method and by the method of the golden section. It should be taken into consideration that the dichotomy method and the method of the golden section refer to methods for searching an extremum of the unimodal functions (that is, functions that have the only extremum over the predefined section of the determination region). That is why the boundaries of the determination region's section containing a single point of the extremum $[t_0, t_k]$ are the initial conditions when calling the subprogram. Fig. 5, a shows a routine implementing the method of dichotomy; Fig. 5, b – the method of the golden section.

For the example considered, Fig. 6 shows the results of computing the limits for the manipulator's grip pole reach under the predefined constraints in the generalized coordinates $q_i(t) \in [q_{i\,min}\ q_{i\,max}]$, $i=1,...,5$ by the method of dichotomy (Fig. 6, a) and the method of the golden section (Fig. 6, b).

$$\text{DihM}(f, t0, dt, tk) := \left| \begin{array}{l} N \leftarrow \dfrac{tk - t0}{dt} \\ \text{for } i \in 1..N \\ \quad \left| \begin{array}{l} x1 \leftarrow t0 + \dfrac{tk - t0 - dt}{2} \\ x2 \leftarrow t0 + \dfrac{tk - t0 + dt}{2} \\ f1 \leftarrow f(x1) \\ f2 \leftarrow f(x2) \\ t0 \leftarrow x1 \text{ if } f2 \geq f1 \\ tk \leftarrow x2 \text{ if } f2 < f1 \\ \text{break if } (tk - t0) \leq dt \end{array} \right. \\ t\_opt \leftarrow \dfrac{(t0 + tk)}{2} \\ f\_max \leftarrow f(t\_opt) \\ \text{MAX} \leftarrow \begin{pmatrix} t\_opt \\ f\_max \end{pmatrix} \end{array} \right.$$

a

$$\text{ZolM}(f, t0, tk, df) := \left| \begin{array}{l} zs \leftarrow 0.618 \\ i \leftarrow 1 \\ t1 \leftarrow tk - (tk - t0) \cdot zs \\ t2 \leftarrow t0 + (tk - t0) \cdot zs \\ f1 \leftarrow f(t1) \\ f2 \leftarrow f(t2) \\ delta \leftarrow tk - t0 \\ \text{while } delta \geq df \\ \quad \left| \begin{array}{l} \text{if } f2 < f1 \\ \quad \left| \begin{array}{l} tk \leftarrow t2 \\ t2 \leftarrow t1 \\ f2 \leftarrow f1 \\ t1 \leftarrow tk - (tk - t0) \cdot zs \\ f1 \leftarrow f(t1) \end{array} \right. \\ \text{if } f2 \geq f1 \\ \quad \left| \begin{array}{l} t0 \leftarrow t1 \\ t1 \leftarrow t2 \\ f1 \leftarrow f2 \\ t2 \leftarrow t0 + (tk - t0) \cdot zs \\ f2 \leftarrow f(t2) \end{array} \right. \\ i \leftarrow i + 1 \\ delta \leftarrow tk - t0 \end{array} \right. \\ t\_opt \leftarrow \dfrac{(tk + t0)}{2} \\ f\_max \leftarrow f(t\_opt) \\ \text{MAX} \leftarrow \begin{pmatrix} t\_opt \\ f\_max \end{pmatrix} \end{array} \right.$$

b

Fig. 5. Subprograms for searching an extremum of the functions f_x, f_y, f_z: a – dichotomy method; b – method of the golden section

4) The following differential equations need to be solved in order to find the highest and lowest value for the coordinates of special point P using the differential calculus methods

$$\frac{dx_p^0}{dt} = \frac{d}{dt} f_x \left(\sin(q_i), \cos(q_i), c_i, t \right) = 0,$$

$$\frac{dy_p^0}{dt} = \frac{d}{dt} f_y \left(\sin(q_i), \cos(q_i), c_i, t \right) = 0,$$

$$\frac{dz_p^0}{dt} = \frac{d}{dt} f_z \left(\sin(q_i), \cos(q_i), c_i, t \right) = 0,$$

where f_x, f_y, f_z are the non-linear dependences of the generalized coordinates $q_i(t)$ on trigonometrical functions; c_i are the geometric parameters of the manipulator design; t is the time.
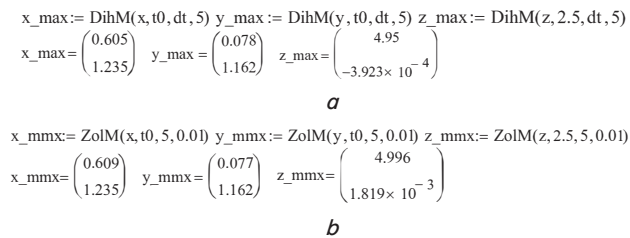
$$\text{x\_max} := \text{DihM}(x, t0, dt, 5) \quad \text{y\_max} := \text{DihM}(y, t0, dt, 5) \quad \text{z\_max} := \text{DihM}(z, 2.5, dt, 5)$$

$$\text{x\_max} = \begin{pmatrix} 0.605 \\ 1.235 \end{pmatrix} \quad \text{y\_max} = \begin{pmatrix} 0.078 \\ 1.162 \end{pmatrix} \quad \text{z\_max} = \begin{pmatrix} 4.95 \\ -3.923 \times 10^{-4} \end{pmatrix}$$

a

$$\text{x\_mmx} := \text{ZolM}(x, t0, 5, 0.01) \quad \text{y\_mmx} := \text{ZolM}(y, t0, 5, 0.01) \quad \text{z\_mmx} := \text{ZolM}(z, 2.5, 5, 0.01)$$

$$\text{x\_mmx} = \begin{pmatrix} 0.609 \\ 1.235 \end{pmatrix} \quad \text{y\_mmx} = \begin{pmatrix} 0.077 \\ 1.162 \end{pmatrix} \quad \text{z\_mmx} = \begin{pmatrix} 4.996 \\ 1.819 \times 10^{-3} \end{pmatrix}$$

b

Fig. 6. The results of computing the limits for the manipulator's grip pole reach under the predefined constraints in the generalized coordinates $q_i(t) \in [q_{i\min}, q_{i\max}]$, $i=1, ..., 5$ by using the Mathcad software application package: *a* – by the dichotomy method; *b* – by the method of the golden section

In a general case, each of the above differential equations can have many solutions. For example, $\dfrac{dx_p^0}{dt} = \dfrac{d}{dt} f_x\left(\sin(q)_i, \cos(q_i), c_i, t\right) = 0$ at $t \in \{t_{x1}, t_{x2}, t_{x3}, t_{x4}, t_{x5}\}$, which means that at points t_{x1}, t_{x2}, t_{x3}, t_{x4}, t_{x5} the function $x_p^0(t)$ has local extrema. To determine global extrema, one must calculate the function $x_p^0(t)$ values for all elements in the set $t \in \{t_{x1}, t_{x2}, t_{x3}, t_{x4}, t_{x5}\}$. The global maximum accepted here is the largest of the local maxima of the function $x_p^0(t)$; the global minimum – the lowest of the local minima.

5) The results of mathematical modeling produced the minimum

$$\vec{r}_{P\min}^0 = \begin{pmatrix} x_{p\min}^0 & y_{p\min}^0 & z_{p\min}^0 & 1 \end{pmatrix}^T$$

and maximum

$$\vec{r}_{P\max}^0 = \begin{pmatrix} x_{p\max}^0 & y_{p\max}^0 & z_{p\max}^0 & 1 \end{pmatrix}^T$$

distance for special point P in the frame of reference associated with the base of the manipulator. The Mathcad software application package provides an opportunity to determine the limits of the reach of the manipulator's grip pole under the predefined constraints in the generalized coordinates $q_i(t) \in [q_{i\min} \ q_{i\max}]$, $i=1,...,5$ using the tracing for charts $x_p^0(t)$, $y_p^0(t)$, $z_p^0(t)$ (Fig. 7).

Based on the results obtained, one can conclude that $x_p^0(t)_{\max} = 1.235$ is achieved at $t=0.6$ s.
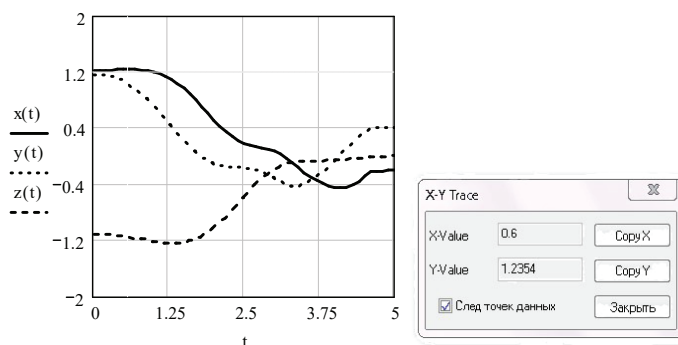

Fig. 7. Computing the limits of the reach of the manipulator grip pole under the predefined constraints in the generalized coordinates $q_i(t) \in [q_{i\min}; q_{i\max}]$, $i=1,...,5$ using the tracing for charts $x_p^0(t)$, $y_p^0(t)$, $z_p^0(t)$

5. 3. Building the boundaries of the manipulator's workspace and identifying the presence of "dead zones" within it

1) The symbolic solution to the first problem of kinematics makes it possible to determine the analytical dependences of the coordinates for special point P in the frame of reference, associated with the base of IR, on the trigonometric functions of generalized coordinates. Fig. 8 shows a fragment of the program for the symbolic solution to the first problem of kinematics.

2) The symbolic solution to the first problem of kinematics using the Mathcad software application package produced the non-linear dependences of the coordinates for special point P in the manipulator base-related reference system in the following form:

$$x_p^0(q_1,q_2,q_3,q_4,q_5,t) = 0.05\cos q_1(t)\cos q_5(t) - $$
$$-0.05\left[\begin{pmatrix} \sin q_1(t)\cos q_2(t)\times \\ \times\cos q_3(t) - \sin q_1(t)\times \\ \times\sin q_2(t)\sin q_3(t) \end{pmatrix}\sin q_4(t) + \\ +\begin{pmatrix} \sin q_1(t)\cos q_2(t)\times \\ \times\sin q_3(t) + \sin q_1(t)\times \\ \times\sin q_2(t)\cos q_3(t) \end{pmatrix}\cos q_4(t)\right]\times$$
$$\times\sin q_5(t) + 0.3\begin{pmatrix} \sin q_1(t)\cos q_2(t)\times \\ \times\cos q_3(t) - \sin q_1(t)\times \\ \times\sin q_2(t)\sin q_3(t) \end{pmatrix}\times$$
$$\times\cos q_4(t) - 0.3\begin{pmatrix} \sin q_1(t)\cos q_2(t)\times \\ \times\sin q_3(t) + \sin q_1(t)\times \\ \times\sin q_2(t)\cos q_3(t) \end{pmatrix}\times$$
$$\times\sin q_4(t) + 0.6\sin q_1(t)\cos q_2(t)\cos q_3(t) - $$
$$-0.6\sin q_1(t)\cdot\sin q_2(t)\cdot\sin q_3(t) + $$
$$+0.7\sin q_1(t)\cdot\cos q_2(t) + 0.8\sin q_1(t);$$

$$y_p^0(q_1,q_2,q_3,q_4,q_5,t) = -0.05(\sin q_1(t)\cos q_5(t) - $$
$$-0.05\left[\begin{pmatrix} \cos q_1(t)\cos q_2(t)\times \\ \times\cos q_3(t) - \cos q_1(t)\times \\ \times\sin q_2(t)\sin q_3(t) \end{pmatrix}\sin q_4(t) + \\ +\begin{pmatrix} \cos q_1(t)\cos q_2(t)\times \\ \times\sin q_3(t) + \cos q_1(t)\times \\ \times\sin q_2(t)\cos q_3(t) \end{pmatrix}\cos q_4(t)\right]\times$$
$$\times\sin q_5(t) + 0.3\begin{pmatrix} \cos q_1(t)\cos q_2\times \\ \times(t)\cos q_3(t) - \cos q_1(t)\times \\ \times\sin q_2(t)\sin q_3(t) \end{pmatrix}\times$$
$$\times\cos q_4(t) - 0.3\begin{pmatrix} \cos q_1(t)\cos q_2(t)\times \\ \times\sin q_3(t) + \cos q_1(t)\times \\ \times\sin q_2(t)\cos q_3(t) \end{pmatrix}\sin q_4(t) + $$
$$+0.6\cos q_1(t)\cos q_2(t)\cos q_3(t) - $$
$$-0.6\cos q_1(t)\sin q_2(t)\sin q_3(t) + $$
$$+0.7\cos q_1(t)\cos q_2(t) + 0.8\cos q_1(t); \tag{1}$$

$$z_p^0(q_1, q_2, q_3, q_4, q_5, t) =$$

$$= -0.05 \left[\begin{pmatrix} -\sin q_2(t) \times \\ \times \cos q_3(t) - \\ -\cos q_2(t) \times \\ \times \sin q_3(t) \end{pmatrix} \times \sin q_4(t) + \\ + \begin{pmatrix} -\sin q_2(t) \times \\ \times \sin q_3(t) + \\ + \cos q_2(t) \times \\ \times \cos q_3(t) \end{pmatrix} \times \cos q_4(t) \right] \times$$

$$\times \sin q_5(t) + 0.3 \begin{pmatrix} -\sin q_2(t) \times \\ \times \cos q_3(t) - \\ -\cos q_2(t) \times \\ \times \sin q_3(t) \end{pmatrix} \times$$

$$\times \cos q_4(t) -$$

$$-0.3 \begin{pmatrix} -\sin q_2(t) \times \\ \times \sin q_3(t) + \\ + \cos q_2(t) \times \\ \times \cos q_3(t) \end{pmatrix} \times$$

$$\times \sin q_4(t) + 0.5 -$$

$$-0.6 \sin q_2(t) \cos q_3(t) -$$

$$-0.6 \cos q_2(t) \cos q_3(t) - 0.7 \sin q_2(t).$$

3) To determine the presence of "dead zones" within the workspace of the manipulator, let us analyze nonlinear dependences (1). The functions of the coordinates for special point P in the frame of reference associated with the base of IR are continuous and differentiated, meaning there are no "dead zones".

4) The projections of the boundaries of the manipulator's work zone onto the coordinate planes in the reference system associated with the base of IR were determined using the Mathcad software application package. Fig. 9 shows a fragment of the program to calculate the boundaries of the manipulator's workspace and to construct its projections onto the *YOZ* plane of the reference system associated with the IR base.

Fig. 10 represents the projection of the boundaries of the manipulator's workspace onto the *YOZ* plane.

5) The boundaries of the manipulator's workspace were determined using the Mathcad software application package. For the manipulator whose kinematic scheme is shown in Fig. 1 the changes in the generalized coordinates $q_i(t) \in [q_{i\,min}; q_{i\,max}]$, $i = 2, 3, 4$ occurs around the OX_i axes, while a change in the generalized coordinate $q_1(t) \in [q_{1\,min}; q_{1\,max}]$ occurs around the OZ_1 axis, and a change in the generalized coordinate $q_5(t) \in [q_{5\,min}; q_{5\,max}]$ occurs around the OY_5 axis. In the three-dimensional Cartesian coordinate system, the boundaries of the working space of a given manipulator represent the surfaces of a complex geometric shape.

When one changes the generalized coordinate q_1 from 0 to 2π radians the working space is a torus whose cross-section is the shape depicted in Fig. 10. If the generalized coordinate q_1 is restricted, the working space of a given manipulator is the corresponding part of the surface of the

said torus. Fig. 11 shows an image of the boundaries of the workspace of the grip pole of the examined manipulator.

.Analiticne_peretvorennya

$$\begin{pmatrix} cq1 & sq1 & 0 & 0 \\ -sq1 & cq1 & 0 & 0 \\ 0 & 0 & 1 & 0.5 \\ 0 & 0 & 0 & 1 \end{pmatrix} \cdot \begin{pmatrix} 1 & 0 & 0 & 0 \\ 0 & cq2 & sq2 & 0.8 \\ 0 & -sq2 & cq2 & 0 \\ 0 & 0 & 0 & 1 \end{pmatrix} \cdot \begin{pmatrix} 1 & 0 & 0 & 0 \\ 0 & cq3 & sq3 & 0.7 \\ 0 & -sq3 & cq3 & 0 \\ 0 & 0 & 0 & 1 \end{pmatrix} \cdot \begin{pmatrix} 1 & 0 & 0 & 0 \\ 0 & cq4 & sq4 & 0.6 \\ 0 & -sq4 & cq4 & 0 \\ 0 & 0 & 0 & 1 \end{pmatrix} \cdot \begin{pmatrix} cq5 & 0 & sq5 & 0 \\ 0 & 1 & 0 & 0 \\ -sq5 & 0 & cq5 & 0 \\ 0 & 0 & 0 & 1 \end{pmatrix} \begin{pmatrix} 0.05 \\ 0.3 \\ 0 \\ 1 \end{pmatrix} \rightarrow$$

$$\rightarrow \begin{bmatrix} 5. \cdot 10^{-2} \cdot cq1 \cdot cq5 - 5. \cdot 10^{-2} \cdot [(sq1 \cdot cq2 \cdot cq3 - sq1 \cdot sq2 \cdot sq3) \cdot sq4 + (sq1 \cdot cq2 \cdot sq3 + sq1 \cdot sq2 \cdot cq3) \cdot cq4] \cdot sq5 + . \\ -5. \cdot 10^{-2} \cdot sq1 \cdot cq5 - 5. \cdot 10^{-2} \cdot [(cq1 \cdot cq2 \cdot cq3 - cq1 \cdot sq2 \cdot sq3) \cdot sq4 + (cq1 \cdot cq2 \cdot sq3 + cq1 \cdot sq2 \cdot cq3) \cdot cq4] \cdot sq5 + \\ -5. \cdot 10^{-2} \cdot [(-sq2 \cdot cq3 - cq2 \cdot sq3) \cdot sq4 + (-sq2 \cdot sq3 + cq2 \cdot cq3) \cdot cq4] \cdot sq5 + . \end{bmatrix}$$

Sqi=Sin(q_i(t)), Cqi=Cos(q_i(t))

Fig. 8. Fragment of the symbolic solution to the first problem of kinematics using the Mathcad software application package

$$qq2 := 0, \frac{\pi}{180} \,.. \, Q2\_max \quad qq3 := 0, \frac{\pi}{180} \,.. \, Q3\_max \quad qq4 := 0, \frac{\pi}{180} \,.. \, Q4\_max$$

$$yy2(qq2) := O\_1_2 + (c12 + c23 + c34) \cdot \cos(qq2)$$
$$yy3(qq3) := O\_2_2 + (c23 + c34) \cdot \cos(qq3 + Q2\_max)$$
$$yy4(qq4) := O\_3_2 + c34 \cdot \cos(qq4 + Q2\_max + Q3\_max)$$
$$yy5(qq3) := O\_1_2 + c12 + (c23 + c34) \cdot \cos(qq3)$$
$$yy6(qq4) := O\_31_2 + c34 \cdot \cos(qq4 + Q3\_max)$$
$$y := -0.15, 0.0001 \,.. \, 0.15$$

$$zz2(qq2) := O\_1_3 + (c12 + c23 + c34) \cdot \sin(qq2)$$
$$zz3(qq3) := O\_2_3 + (c23 + c34) \cdot \sin(qq3 + Q2\_max)$$
$$zz4(qq4) := O\_3_3 + c34 \cdot \sin(qq4 + Q2\_max + Q3\_max)$$
$$zz5(qq3) := O\_1_3 + (c23 + c34) \cdot \sin(qq3)$$
$$zz6(qq4) := O\_31_3 + c34 \cdot \sin(qq4 + Q3\_max)$$
$$z(y) := \sqrt{0.15^2 + 0.137^2 - y^2}$$

$$zz2(0) = 0.05 \quad zz3(0) = 1.869 \quad zz2(QQ2\_max) = 1.869 \quad zz3(Q3\_max) = -0.383$$
$$zz4(0) = -0.383 \quad zz5(0) = 0.05 \quad z(-0.15) = 0.137 \quad z(0.15) = 0.137$$
$$zz4(Q4\_max) = 0.137 \quad zz6(0) = 1.176 \quad zz6(Q4\_max) = 0.137$$

$$yy2(0) = 2.1 \quad yy2(QQ2\_max) = -1.05 \quad yy3(0) = -1.05$$
$$yy3(Q3\_max) = -1.05 \quad yy4(0) = -1.05 \quad yy5(0) = 2.1$$
$$yy4(Q4\_max) = -0.15 \quad yy6(0) = 0.15 \quad yy6(Q4\_max) = 0.15$$

Fig. 9. A snippet of the program to calculate the boundaries of the workspace of the manipulator grip pole under the predefined constraints in the generalized coordinates $q_i(t) \in [q_{i\,min}; q_{i\,max}]$, $i = 1,...,5$ using the Mathcad software application package
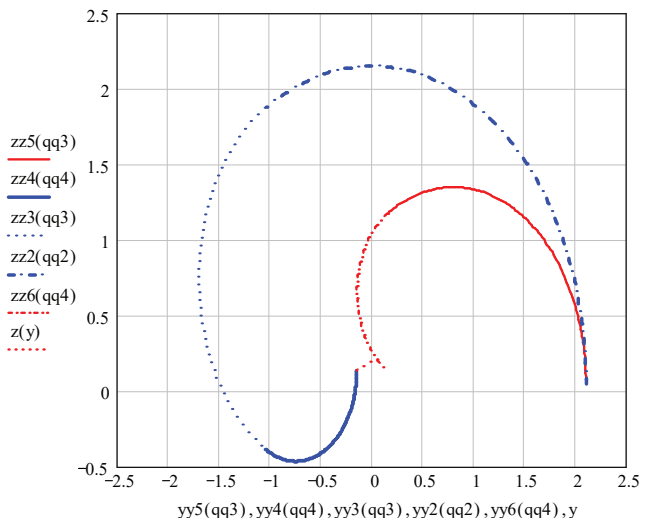

Fig. 10. Projection onto the *YOZ* plane of the boundaries of the workspace of the manipulator grip pole under the specified constraints in the generalized coordinates $q_i(t) \in [q_{i\,min}; q_{i\,max}]$, $i = 1,...,5$ using the Mathcad software application package
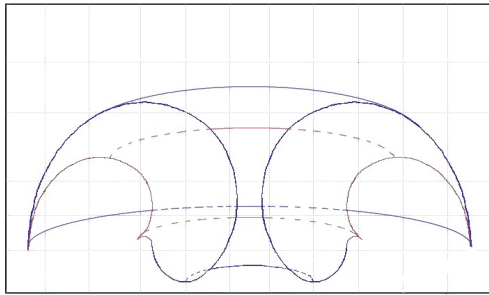
Fig. 11. The boundaries of the workspace of the manipulator grip pole under the predefined constraints in the generalized coordinates $q_i(t) \in [q_{i\,min}; q_{i\,max}]$, $i=1,...,5$ using the Mathcad software application package

6. Discussion of results of studying the workspace of a manipulator using Mathcad

The obstacles within the workspace of manipulators are registered by a sensor system and processed by the control system. In order to avoid collisions, no-go zones are formed within the workspace. Solving the inverse problem of kinematics establishes in the forbidden zones of the workspace a set of unacceptable configurations of the manipulator as the sets of prohibited values of the generalized coordinates. Consequently, the region of determining the values of generalized coordinates, if there are obstacles within the workspace of the manipulator, narrows and could be set by intervals $q_i(t) \in [q_{i\,min}; q_{i\,max}]$, $i=1,...n$. The drive of mobility degree generates a build-up of the generalized coordinate according to the law $Q_i(t)=f(a_i,b_i,t,q_{i0})$. The actual implementation of $q_i(t)$ takes into consideration the drive-generated law of change in the generalized coordinate, the design features of the kinematic pair, and the constraints $q_i(t) \in [q_{i\,min}; q_{i\,max}]$. Fig. 2, a shows a fragment of the program that models the law of changing the generalized coordinate $q_3(t)$ taking into consideration the constraints. The charts of the change in the estimated $Q_3(t)$ and actual $q_3(t)$ values of the generalized coordinate are shown in Fig. 2b. If, under these conditions, the manipulator must perform programmed technological operations, the control system performs a synthesis of the trajectory based on a digital model of the current state of the workspace taking into consideration the inaccessibility of forbidden zones, unacceptable configurations, and generalized coordinates.

Sometimes, during the execution of technological operations, there is partial jamming of the kinematic pair; the power of the drive is not enough to implement the planned law of changing the generalized coordinate, or the actual friction factor in the drive does not provide for the required increment in the generalized coordinate. In this case, it is necessary to determine by a programming method the laws of changing the generalized coordinates $q_i(t)$ taking the constraints into consideration. For the example considered, a fragment of the program to model the laws of changing the generalized coordinates of the manipulator taking into consideration the predefined constraints for the movement of the grip pole is shown in Fig. 3. In order to maintain the functionality of the manipulator, trajectory synthesis is performed considering the above constraints. The actual implementation of $q_i(t)$ takes into consideration the drive-generated law of change in the generalized coordinate $Q_i(t)$ at the specified power and friction factor, the design features of the kinematic pair, and the constraint $q_i(t) \in [q_{i\,min}; q_{i\,max}]$.

The simulation of the manipulator's movement was conducted in the Mathcad environment for different load variants, different sequences of movements, and laws of change in the generalized coordinates. That has made it possible to analyze the acceptable configurations of the manipulator, synthesize the trajectories of the grip, and choose the optimal trajectory. For the considered example, the results of the simulation of the movement of the grip pole are shown in Fig. 4.

The limits of reach for special point P could be found by using the methods to search for an extremum of unimodal functions by applying differential calculus methods, or numerically, by employing the tracing for charts $x_p^0(t), y_p^0(t), z_p^0(t)$.

To find the highest and smallest value of the coordinates for special point P, routines have been developed to calculate an extremum of the functions f_x, f_y, f_z by a dichotomy method and by the method of the golden section. Fig. 5a shows a routine implementing the method of dichotomy; Fig. 5, b – the method of the golden section. It should be taken into consideration that the dichotomy method and the method of the golden section refer to methods that search for an extremum of unimodal functions (that is the functions that have the only extremum over a predefined section of the determination region). That is why the boundaries of the determination region's section containing a single point of the extremum $[t_0, t_k]$ are the initial conditions when calling the routine. For the example considered, Fig. 6 shows the results of searching for the highest and least value of the coordinates for special point P under the specified constraints by the method of dichotomy (Fig. 6, a) and the method of the golden section (Fig. 6, b).

When tracing the charts $x_p^0(t), y_p^0(t), z_p^0(t)$, the user "through the peephole" determines the point of an extremum, so this method cannot be considered reliable. Fig. 7 shows the results of calculating the limits of the reach of the grip pole of the manipulator under the specified constraints in the generalized coordinates $q_i(t) \in [q_{i\,min}; q_{i\,max}]$, $i=1,...,5$ using the tracing for charts $x_p^0(t), y_p^0(t), z_p^0(t)$. Calculating the limits of the reach by the grip pole implies using the methods to find an extremum of the unimodal functions by applying differential calculus techniques, or numerically, using the tracing for graphs $x_p^0(t), y_p^0(t), z_p^0(t)$. To reduce the error and eliminate the subjectivity of the assessment, I have compiled subprograms to calculate the limits of grip in several ways to verify the results.

To determine the presence of "dead zones" within a workspace of the manipulator, the nonlinear dependences (1) were analyzed to calculate the coordinates for special point P in the frame of reference associated with the base of the manipulator. Since functions (1) are continuous and differentiated, it was concluded that there are no "dead zones". It should be noted that formulae (1) could be derived on the basis of the symbolic solution to the first problem of kinematics using the Mathcad software application package. A fragment of the symbolic solution to the first problem of kinematics using the Mathcad software application package is shown in Fig. 8.

Since the kinematic IR scheme typically contains at least five degrees of mobility, in the three-dimensional Cartesian system the boundaries of the work zone represent the surfaces of a complex geometric shape. It is proposed to consider projections of the boundaries of the manipulator's work zone onto the coordinate planes in the frame of reference associated with the base of the robot. A routine in Mathcad has been developed to calculate the boundaries of the ma-

nipulator's workspace and build its projections. Fig. 9 shows a fragment of the program to calculate the boundaries of the workspace of the pole of the manipulator's grip under the predefined constraints. Fig. 10 shows a representation of the projection of the boundaries of the workspace of the pole of the manipulator's grip under the predefined constraints onto the *YOZ* plane in the frame of reference associated with the base of the robot.

In a three-dimensional Cartesian coordinate system, the boundaries of the working space of a given manipulator represent a part of the surface of the torus. Fig. 11 shows a representation of the boundaries of the workspace of the gripping pole of the manipulator in question.

It should be noted that programming languages (Fortran (USA), Pascal (Switzerland), C (USA) or mathematical packages (MATLAB (USA), Mathcad (USA) could be used to analyze the current state of the workspace on a computer.

To effectively use the devised method, a manipulator must be equipped with a sensor system that generates operational and reliable information about the environment. Otherwise, the need to verify primary information from sensors reduces performance and distorts the digital model of the current state of the workspace.

Since the actual implementation of the generalized coordinates $q_i(t)$ and the coordinate of the manipulator's grip pole $x_p^0(t)$, $y_p^0(t)$, $z_p^0(t)$ are the functions of time, at the implementation phase of the method it is necessary to adjust the discretion of the sensor survey, the step of the program implementation, and the minimum time necessary for the manipulator to avoid obstacles. Otherwise, acquiring and processing information, calculating the boundaries of the manipulator's workspace, planning the trajectory of the workaround, synthesis, and the implementation of the relevant law of change in the generalized coordinates may take too long and would not avoid a collision.

When applying the devised method for manipulative MR, it should be taken into consideration that the boundaries of the workspace are defined in the frame of reference associated with the base of the robot placed on a mobile platform. Therefore, the planning of the trajectory of the workaround, the choice of acceptable configurations of the manipulator, the synthesis of the optimal trajectory of the manipulator grip should be carried out taking into consideration the degrees of mobility and accuracy of the positioning of the platform.

When advancing the proposed method, it is advisable to refine a three-dimensional representation of the boundaries of the manipulator's workspace using the Mathcad software application package. One should take into consideration, in this case, certain constraints of the Mathcad's graphics capabilities.

7. Conclusions

1. The actual laws of change in the generalized coordinates $q_i(t)$ have been defined, taking into consideration constraints in the kinematic pairs, the power of drives, and friction ratios. A routine in Mathcad has been developed to simulate the movement of the manipulator taking the above constraints into consideration. Based on the data obtained, the current state of the set of unacceptable manipulator configurations is determined, as the sets of prohibited values for the generalized coordinates.

2 The limits of grip reach in the presence of restrictions and obstacles in the workspace of the manipulator were calculated in the Mathcad environment. In this case, programmatically, based on the sets of forbidden values for the generalized coordinates, unattainable points or forbidden zones of the working space are identified.

3. The construction of the boundaries of the manipulator's workspace and the detection of the presence of "dead zones" within it was carried out using the Mathcad software application package. This could make it possible to synthesize the optimal trajectory taking into consideration the prohibited regions within the workspace and the set of acceptable configurations of the manipulator, as well as ensure the orientation and accuracy of grip positioning.

Acknowledgments

References

1. Grigoriev, S. N., Andreev, A. G., Ivanovsky, S. P. (2013). Present State and Prospects of Industrial Robotics. Mehatronika, avtomatizatsiya, upravlenie, 1, 30–34.

2. Schwandt, A., Yuschenko, A. S. (2013). Industrial robot application for advanced mechanical shaping technologies. Robototehnika i tehnicheskaya kibernetika, 1 (1), 18–21.

3. Tang, M., Gu, Y., Wang, S., Liang, Q., Wang, X. (2019). Planning of safe working space for the hot-line working robot ICBot. International Journal of Applied Electromagnetics and Mechanics, 61 (1), 97–110. doi: https://doi.org/10.3233/jae-180057

4. Hou, R. G., Gao, J., Li, Z. Y., Wang, S. J., Zhao, G. Y. (2012). Analysis of the Movable Cotton Robot Palletizer Working Space Based on Graphing Method. Advanced Materials Research, 500, 454–459. doi: https://doi.org/10.4028/www.scientific.net/amr.500.454

5. Goritov, A. N. (2017). Building a three-dimensional model of the workspace of an industrial robot. Proceedings of Tomsk State University of Control Systems and Radioelectronics, 20 (4), 117–121. doi: https://doi.org/10.21293/1818-0442-2017-20-4-117-121

6. Antoshkin, S. B., Bakanov, M. V., Sizykh, V. N. (2019). An autonomous robot control system based on an inverse problems method in dynamics. Modern Technologies. System Analysis. Modeling, 62 (2), 15–23. doi: https://doi.org/10.26731/1813-9108.2019.2(62).15-23

7. Khomchenko, V. G. (2018). About ways of the task of orientation of the working body of the robot manipulator. Dynamics of Systems, Mechanisms and Machines, 6 (2), 76–81. doi: https://doi.org/10.25206/2310-9793-2018-6-2-76-81

8. He, B., He, X. L., Han, L. Z., Cao, J. T., Li, M., Tian, Y. Z. (2010). Working Space Analysis and Simulation of Modular Service Robot Arm Based on Monte Carlo Method. Applied Mechanics and Materials, 34-35, 1104–1108. doi: https://doi.org/10.4028/www.scientific.net/amm.34-35.1104

9. Lopatin, P. K. (2012). Algoritm issledovaniya dostizhimosti obekta manipulyatorom v neizvestnoy srede. Mehanotronika, avtomatizatsiya, upravlenie, 9, 49–52.

10. Lopatin, P. (2019). Manipulator control in an unknown static environment. Robotics and Technical Cybernetics, 7 (1), 58–64. doi: https://doi.org/10.31776/rtcj.7108

11. Xie, B. (2012). Motion Planning of Reaching Point Movements for 7R Robotic Manipulators in Obstacle Environment Based on Rapidly-exploring Random Tree Algorithm. Journal of Mechanical Engineering, 48 (03), 63. doi: https://doi.org/10.3901/jme.2012.03.063

12. Schwandt, A., Yuschenko, A. (2020). Collaborative manipulation robots programming with the use of augmented reality interface. Robotics and Technical Cybernetics, 8 (2), 139–149. doi: https://doi.org/10.31776/rtcj.8205

13. Pritykin, F. N., Nefedov, D. E. (2016). Study of the Surfaces Defining the Area Boundaries of the Allowable Configurations of the Mobile Manipulator Mechanism with the Available Forbidden Zones. Mehatronika, Avtomatizacia, Upravlenie, 17 (6), 407–413. doi: https://doi.org/10.17587/mau.17.407-413

14. Pritykin, F. N., Nefedov, D. I. (2018). Creating a knowledge base about past experience in the synthesis of arm movements of an android robot based on the use of the area of allowed configurations. Software systems and computational methods, 4, 60–67. doi: https://doi.org/10.7256/2454-0714.2018.4.26638

15. Karavaev, Yu. L., Shestakov, V. A. (2018). Construction of a Service Area of a Highly Maneuverable Mobile Manipulation Robot. Intelligent Systems in Manufacturing, 16 (3), 90–96. doi: https://doi.org/10.22213/2410-9304-2018-3-90-96

16. Li, W., Xiong, R. (2019). Dynamical Obstacle Avoidance of Task- Constrained Mobile Manipulation Using Model Predictive Control. IEEE Access, 7, 88301–88311. doi: https://doi.org/10.1109/access.2019.2925428

17. Krasnov, A. Y., Chepinskiy, S. A., Yifan, C., Huimin, L., Kholunin, S. A. (2017). Trajectory control for a robot motion in presense of moving obstacles. Scientific and Technical Journal of Information Technologies, Mechanics and Optics, 17 (5), 790–797. doi: https://doi.org/10.17586/2226-1494-2017-17-5-790-797

18. Korsakov, A., Astapova, L., Smirnova, E. (2020). Object-oriented reconstruction of manipulator's working area by point cloud. Robotics and Technical Cybernetics, 8 (3), 198–205. doi: https://doi.org/10.31776/rtcj.8305

19. Ashchepkova, N. (2015). Mathcad in the kinematic and dynamic analysis of the manipulator. Eastern-European Journal of Enterprise Technologies, 5 (7 (77)), 54–63. doi: https://doi.org/10.15587/1729-4061.2015.51105

20. Kolyubin, S. A. (2017). Dinamika robototehnicheskih sistem. Sankt-Peterburg: Universitet ITMO, 117.

21. Maxfield, B. (2009). Essential Mathcad for Engineering, Science, and Math. Academic Press, 528. doi: https://doi.org/10.1016/b978-0-12-374783-9.x0001-x

22. Yurevich, E. I. (2017). Osnovy robototehniki. Sankt-Peterburg: BHV-Peterburg, 304.